Preprints.org

Article

Not peer-reviewed version

Latency-Constrained UAV Operations over SATCOM: A System-Level Analytical Framework Incorporating Stochastic Jitter Modelling, Adaptive Autonomy, and Regulatory Consolidation

Nick Barua *

Posted Date: 20 April 2026

doi: 10.20944/preprints202604.1322.v1

Keywords: UAV; SATCOM; latency; beyond-line-of-sight; stochastic jitter; teleoperation; adaptive autonomy; GEO; LEO; probability of safety breach; unmanned aerial systems; regulatory standards

Preprints.org is a free multidisciplinary platform providing preprint service that is dedicated to making early versions of research outputs permanently available and citable. Preprints posted at Preprints.org appear in Web of Science, Crossref, Google Scholar, Scilit, Europe PMC.

Copyright: This open access article is published under a Creative Commons CC BY 4.0 license, which permit the free download, distribution, and reuse, provided that the author and preprint are cited in any reuse.

Preprints.org (www.preprints.org) | NOT PEER-REVIEWED | Posted: 20 April 2026 doi:10.20944/preprints202604.1322.v1

Disclaimer/Publisher's Note: The statements, opinions, and data contained in all publications are solely those of the individual author(s) and contributor(s) and not of MDPI and/or the editor(s). MDPI and/or the editor(s) disclaim responsibility for any injury to people or property resulting from any ideas, methods, instructions, or products referred to in the content.

Article

Latency-Constrained UAV Operations over SATCOM: A System-Level Analytical Framework Incorporating Stochastic Jitter Modelling, Adaptive Autonomy, and Regulatory Consolidation

Nick Barua

Chairman & CEO, AN Holdings Co., Visiting Professor, Shiga University of Medical Science, Kobe Gakuin University, Japan; s.nick.barua@gmail.com

Abstract

Satellite communication (SATCOM) has emerged as a critical enabler of beyond-line-of-sight (BLOS) unmanned aerial vehicle (UAV) operations, yet its role as a constraining factor on UAV control performance and mission safety has received insufficient analytical treatment. This paper presents a comprehensive, system-level analytical framework that models end-to-end communication latency across the SATCOM pipeline and directly links it to UAV control responsiveness, mission safety, and autonomy requirements. The framework proceeds through four integrated contributions. First, a deterministic latency decomposition model establishes governing equations that define the critical velocity threshold and the autonomy transition boundary for human-in-the-loop UAV teleoperation. Second, this deterministic model is extended into a probabilistic framework by incorporating stochastic jitter arising from low-earth orbit (LEO) satellite handovers, enabling the derivation of a probability of safety breach metric that replaces binary operational thresholds with continuous risk quantification. Third, an adaptive autonomy control architecture is proposed, in which UAV systems monitor real-time link performance and dynamically adjust velocity and control authority in response to measured latency conditions. Fourth, the regulatory implications of the framework are examined, identifying pathways toward latency-aware UAV operational standards. Across three representative operational scenarios—urban surveillance, remote infrastructure inspection, and disaster response—the results demonstrate that geostationary earth orbit (GEO) SATCOM constrains safe teleoperation to low-speed regimes, while LEO constellations extend the operable envelope but introduce jitter-driven risk. The proposed framework provides a principled, durable basis for communication architecture selection, autonomy system design, and the development of latency-aware standards for next-generation unmanned aerial systems.

Keywords: UAV; SATCOM; latency; beyond-line-of-sight; stochastic jitter; teleoperation; adaptive autonomy; GEO; LEO; probability of safety breach; unmanned aerial systems; regulatory standards

1. Introduction

The proliferation of unmanned aerial vehicles across civil, commercial, and defence domains has fundamentally altered the landscape of aerial operations. UAVs now serve critical roles in surveillance, infrastructure inspection, precision agriculture, disaster response, and logistics delivery, with global deployment trajectories indicating continued expansion throughout the coming decade [1]. Central to the utility of these platforms is their capacity to operate beyond the visual line of sight of their operators—a capability that is almost entirely dependent upon reliable, long-range communication links [2].

Satellite communication has been identified as the principal technology enabling BLOS UAV operations, providing connectivity across geographical areas where terrestrial networks are

© 2026 by the author(s). Distributed under a Creative Commons CC BY license.

Preprints.org (www.preprints.org) | NOT PEER-REVIEWED | Posted: 20 April 2026 doi:10.20944/preprints202604.1322.v1

unavailable or unreliable [3]. Previous work by the author established the foundational importance of SATCOM as a communication backbone for UAV systems, demonstrating that satellite links can support the transmission of intelligence, surveillance, and reconnaissance (ISR) data in near-real-time, extending the operational envelope of unmanned platforms far beyond conventional radio-frequency constraints [4]. Subsequent analysis of the global homeland security satellite imagery market further reinforced the strategic convergence of spaceborne communication, Earth observation, and unmanned systems within national security and civil protection frameworks [5].

While the enabling role of SATCOM is well established, its constraining influence on UAV operational performance has received comparatively limited analytical treatment. Satellite communication inherently introduces latency into the control loop—arising from signal propagation, transponder processing, ground segment handling, and return-path delays [6]. For geostationary satellites at approximately 35,786 kilometres, one-way propagation delay approaches 270 milliseconds, yielding round-trip times exceeding 600 milliseconds once processing delays are included [7]. Such delays impose fundamental constraints on operator responsiveness, closed-loop control stability, and the viability of real-time decision-making [8].

The emergence of low-earth orbit (LEO) satellite constellations has introduced substantially reduced propagation delays, with one-way latencies potentially below 20 ms [9]. However, LEO systems introduce a further challenge: stochastic jitter arising from frequent orbital handovers. This variability is not captured by deterministic latency models and constitutes a distinct, undercharacterised risk to UAV control stability. Concurrently, fifth-generation (5G) terrestrial networks offer ultra-low latency within areas of coverage but lack the geographic reach essential for BLOS operations [10].

The present paper addresses the analytical gap by developing a four-part framework. First, it establishes a deterministic latency decomposition and derives practical operational thresholds. Second, it extends this model probabilistically, incorporating LEO jitter to compute a quantitative probability of safety breach. Third, it translates these thresholds into an adaptive autonomy control architecture capable of real-time response to measured link conditions. Fourth, it examines the regulatory implications and pathways toward standardisation. Throughout, the contribution is positioned at the system level—providing a durable framework that remains applicable regardless of advances in individual communication or perception technologies.

The remainder of this paper is organised as follows. Section 2 provides background on SATCOM-enabled UAV communication. Section 3 presents the deterministic and stochastic latency models. Section 4 reports the results and latency threshold analysis. Section 5 introduces the adaptive autonomy control framework. Section 6 outlines the empirical validation methodology. Section 7 examines regulatory implications. Section 8 provides a discussion, and Section 9 concludes with design recommendations and future directions.

2. Background

2.1. Satellite Communication for UAV Operations

Satellite communication systems provide the essential data relay infrastructure for UAV operations conducted beyond the reach of terrestrial line-of-sight links. The architecture comprises three segments: the space segment (satellite transponders), the ground segment (ground control stations and gateway earth stations), and the user segment (UAV-mounted terminals) [6]. Data flows bidirectionally: uplink transmissions carry command and control signals from the ground operator to the UAV, while downlink transmissions return telemetry, video, and sensor data [3].

Barua [4] established that SATCOM is positioned to become the dominant communication paradigm for persistent BLOS UAV operations, demonstrating its applicability across ISR transmission, payload delivery, and traffic monitoring. That work highlighted the particular importance of SATCOM for high-altitude long-endurance (HALE) and high-altitude platform station (HAPS) configurations. Further work by Barua [5] The global homeland security satellite imagery

© 2026 by the author(s). Distributed under a Creative Commons CC BY license.

Preprints.org (www.preprints.org) | NOT PEER-REVIEWED | Posted: 20 April 2026 doi:10.20944/preprints202604.1322.v1

market reinforced the strategic convergence of spaceborne assets and unmanned systems within civil protection frameworks.

2.2. Latency in Satellite Communication Systems

GEO satellites at approximately 35,786 kilometres provide continuous wide-area coverage but impose one-way propagation delays of 240 to 280 milliseconds, yielding round-trip times of 480 to 560 milliseconds before processing delays are considered [7]. These delays are physically irreducible. LEO satellites at 500 to 2,000 kilometres offer one-way latencies of 5 to 20 milliseconds, but require large constellations and introduce frequent handovers [9]. Modern LEO constellations address this through dense orbital planes and inter-satellite laser links, but handover-induced latency spikes—the jitter central to Phase 1 of this framework—remain an active engineering challenge [11]. Medium Earth Orbit (MEO) satellites occupy an intermediate position, offering one-way latencies of approximately 70 to 130 milliseconds [6].

2.3. UAV Control Under Communication Delay

The relationship between communication delay and control performance has been extensively studied in teleoperation and networked control systems [8]. When an operator controls a remote vehicle through a delayed link, the state information received is already outdated by the round-trip delay. As delay increases, tracking error grows, obstacle avoidance degrades, and effective control is ultimately lost [12]. Research in networked control has established that closed-loop stability depends on both the magnitude and variability of the delay [12]. For UAV operations, this translates to a practical constraint: the total reaction time of the human–UAV control loop must remain below a mission-dependent threshold, beyond which autonomy becomes necessary [13].

2.4. Terrestrial Alternatives and Hybrid Architectures

Fifth-generation cellular networks offer theoretical end-to-end latencies below 10 milliseconds, making them attractive for UAV control within coverage areas [10]. However, 5G connectivity at UAV altitudes introduces cell-edge interference and handover challenges [14]. Practical Beyond-Line-of-Sight (BLOS) deployments increasingly employ hybrid architectures combining 5G for low-latency control within coverage and SATCOM for extended-range segments. The framework presented herein accommodates such hybrid configurations by modelling latency as a function of the active communication mode at any given mission phase.

3. Section Title

3.1. Deterministic End-to-End Latency Model

The framework begins with a decomposition of the total end-to-end communication delay within the SATCOM pipeline, as illustrated in Figure 1. The total latency experienced in a single command–response cycle is expressed as:

$$T_{\text{total}} = T_{\text{uplink}} + T_{\text{satellite}} + T_{\text{processing}} + T_{\text{downlink}} \quad (1)$$

where T_{up}^{Link} is the propagation delay from the ground control station to the satellite; $T_{sat}^{eLLI_t^e}$ is the transponder processing delay; $T_{p^r_o{}^{ce}_{ss}}^{Ink}$ is the ground segment processing delay encompassing demodulation, decryption, and routing; and $T^{d}_{o}{}^{WnLInk}$ is the propagation delay from the satellite to the UAV terminal. For GEO at nadir, the uplink and downlink propagation delays are each approximately 119.4 milliseconds, based on an orbital altitude of 35,786 km and the speed of light at 2.998×10^8 m/s.

© 2026 by the author(s). Distributed under a Creative Commons CC BY license.

Preprints.org (www.preprints.org) | NOT PEER-REVIEWED | Posted: 20 April 2026 doi:10.20944/preprints202604.1322.v1

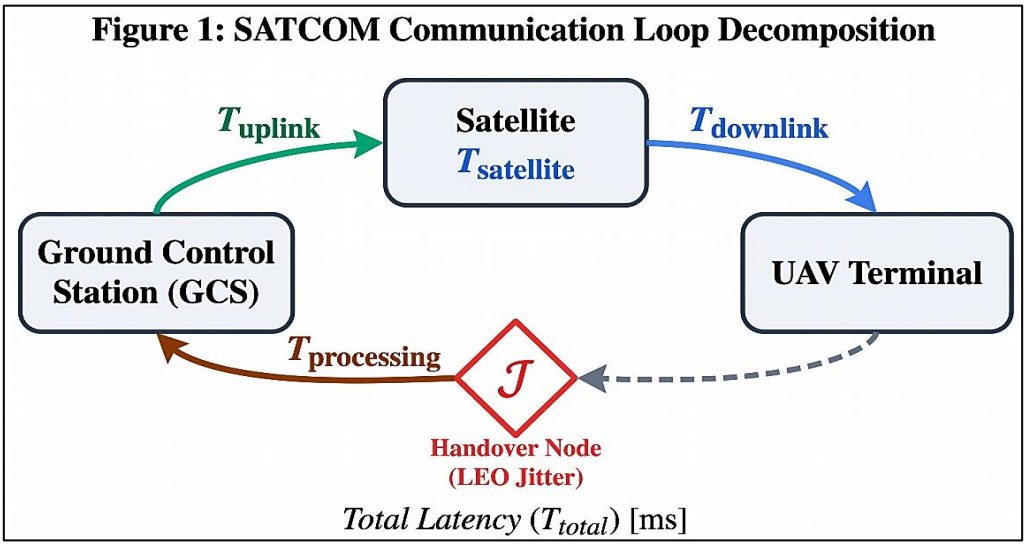

Figure 1. Block diagram of the SATCOM communication loop, illustrating the sequential delay components (T_{up}^{LPk}, T_{sat}^{eLLIe}, $T_{p}^{r}{}_{o}^{ce}{}_{ss}^{Pk}$, $T^{d}{}_{o}^{WnLPk}$) within the full bidirectional command–response cycle as defined in Equation (1). The stochastic jitter component $\mathcal{J}$ is indicated at the LEO handover transition node.

3.2. Reaction Time Model and Critical Velocity

The total reaction time of the human–UAV control loop includes the operator's cognitive and motor response time:

$$T_{reaction} = T_{total} + T_{human} \quad (2)$$

where $T^{h}{}_{uva}^{n}$ represents the operator's perception-to-action delay, typically 200 to 300 milliseconds for trained UAV pilots [12]. The minimum reaction distance for a UAV at velocity v is:

$$d_{reaction} = v \times T_{reaction} \quad (3)$$

This establishes a direct link between communication latency and operational safety. The critical velocity—the maximum UAV speed at which safe operation can be maintained—is:

$$v_{critical} = d_{safe} / (T_{total} + T_{human}) \quad (4)$$

As latency increases, $v^{crI}{}_{t}^{Ic}{}_{a}^{L}$ decreases, progressively restricting the mission envelope. The autonomy transition threshold—the latency at which $v^{crI}{}_{t}^{Ic}{}_{a}^{L}$ equals the minimum required mission velocity v^{mIn}—is:

$$T_{total,threshold} = (d_{safe} / v_{min}) - T_{human} \quad (5)$$

For latencies below this threshold, human teleoperation is viable. Above it, autonomous or semi-autonomous operation is required.

3.3. Stochastic Extension: LEO Jitter Modelling

The deterministic model of Equations (1)–(5) treats T_{tota}^{L} as a fixed quantity. In practice, LEO satellite systems introduce stochastic variability in latency, arising primarily from handover events between successive orbital passes. During a handover, the signal path transitions between satellites, introducing a transient latency spike that is neither predictable in magnitude nor duration from a deterministic standpoint. This jitter component, denoted $\mathcal{J}$, is modelled as a zero-mean random variable with variance $\sigma^2\mathcal{J}$, characterised empirically from LEO constellation performance data [9,11]. The stochastic reaction time becomes:

$$T_{reaction} = (T_{total} + \mathcal{J}) + T_{human} \quad (6)$$

where $\mathcal{J}$ represents the stochastic jitter variable. The distribution of $\mathcal{J}$ is modelled as log-normal rather than Gaussian, reflecting the asymmetric nature of handover-induced spikes: delays cannot be negative, but can extend substantially above the mean during multi-satellite transition events. This

© 2026 by the author(s). Distributed under a Creative Commons CC BY license.

Preprints.org (www.preprints.org) | NOT PEER-REVIEWED | Posted: 20 April 2026 doi:10.20944/preprints202604.1322.v1

choice is consistent with empirical latency distributions reported for LEO communication systems [9].

3.4. Probability of Safety Breach

The stochastic extension enables the computation of a probability of safety breach (Pbreach), defined as the probability that the stochastic reaction time exceeds the safe operating threshold for a given mission velocity and safe separation distance:

$$P_{breach} = P(\mathcal{J} > \Delta T_{margin}) \quad (7)$$

where ΔT_{margin} is the latency safety margin, defined as the difference between the deterministic autonomy transition threshold (Equation (5)) and the nominal T_{total}:

$$\Delta T_{margin} = T_{total,threshold} - T_{total,nominal} \quad (8)$$

For a log-normal jitter distribution with parameters $\mu\mathcal{J}$ and $\sigma\mathcal{J}$, Pbreach is computed directly from the complementary cumulative distribution function. This transforms the binary Zone A/B/C boundary into a continuous risk gradient: as nominal latency approaches the threshold, Pbreach rises, quantifying the probability that any given handover event will push the system into an unsafe operating condition. A system design target of Pbreach $\leq 10^{-6}$ per flight hour is proposed, consistent with aviation safety standards for catastrophic event probabilities [13].

3.5. Analytical Parameters

The framework is evaluated across three communication modes and three operational scenarios. Latency parameters are summarised in Table 1. Operational scenario parameters are presented in Table 2. A representative human response time of T_{human} = 250 ms and jitter standard deviation of $\sigma\mathcal{J}$ = 35 ms (consistent with reported LEO handover characteristics [11]) are used throughout. The communication latency across different systems is summarised in Table 1.

Table 1. Typical Latency Parameters by Communication Mode.

Communication Mode	One-Way Propagation Delay (ms)	Satellite/Network Processing (ms)	Ground Processing (ms)	Round-Trip T_{total} (ms)	Typical $\sigma\mathcal{J}$ (ms)
GEO SATCOM	240–280	5–50	10–100	540–750	N/A
LEO SATCOM	5–20	2–30	10–50	25–140	20–60
5G Terrestrial	< 1	1–5	2–10	5–20	< 2

Sources: Compiled from [6,7,9–11].

The model parameters and their definitions are presented in Table 2.

Table 2. Operational Scenario Parameters.

Scenario	UAV Speed Range (m/s)	d_{safe} (m)	v^{min} (m/s)	T_{total}, threshold @ v^{min} (s)	Primary Comm. Mode
Urban Surveillance	10–25	30	10	2.750	5G / LEO
Remote Inspection	15–40	50	15	3.083	GEO / LEO
Disaster Response	20–50	20	20	0.750	LEO / GEO

4. Results and Analysis

4.1. Deterministic Latency Threshold Analysis

Applying Equation (5) with T_{uvan}^{h} = 250 ms, the autonomy transition thresholds for each scenario confirm the operational boundaries set out in Table 2. For urban surveillance at minimum mission speed (v^{min} = 10 m/s), the threshold of 2.750 seconds permits GEO SATCOM teleoperation with an

© 2026 by the author(s). Distributed under a Creative Commons CC BY license.

Preprints.org (www.preprints.org) | NOT PEER-REVIEWED | Posted: 20 April 2026 doi:10.20944/preprints202604.1322.v1

adequate margin. However, at full operational speed (v = 25 m/s), the threshold falls to 0.950 seconds, leaving a negligible margin for GEO SATCOM and placing the system at the boundary of reliable teleoperation. Any additional delay from atmospheric fading or network congestion would breach this limit.

For remote inspection at v^{min} = 15 m/s, the threshold of 3.083 seconds accommodates GEO SATCOM comfortably. At v = 40 m/s, the threshold reduces to 1.000 seconds, remaining within the feasible GEO envelope but with limited margin. For disaster response—the most demanding scenario—the threshold of 0.750 seconds at v^{min} = 20 m/s can only marginally be satisfied by GEO SATCOM under ideal conditions. At v = 50 m/s, the threshold falls to 0.150 seconds, which is below the physical minimum of GEO SATCOM and at the upper boundary of LEO capability, confirming that full autonomous operation is required at high speeds in this scenario.

4.2. Stochastic Analysis and Probability of Safety Breach

Figure 2 illustrates both the deterministic control effectiveness curves and the stochastic confidence bands arising from LEO jitter. For LEO SATCOM at a nominal T_{total}^{L} of 80 ms and σ_J = 35 ms, the latency safety margin ΔT_{a}^{max} for the disaster-response scenario at v = 25 m/s is approximately 70 ms. Substituting into Equation (7) with a log-normal distribution yields Pbreach ≈ 2.3 × 10^{-2}—a probability that is non-trivial and substantially above the proposed safety target of 10^{-6} per flight hour. This demonstrates that, even for LEO SATCOM, handover jitter alone is sufficient to introduce meaningful safety risk in high-speed, high-criticality scenarios without compensatory measures.

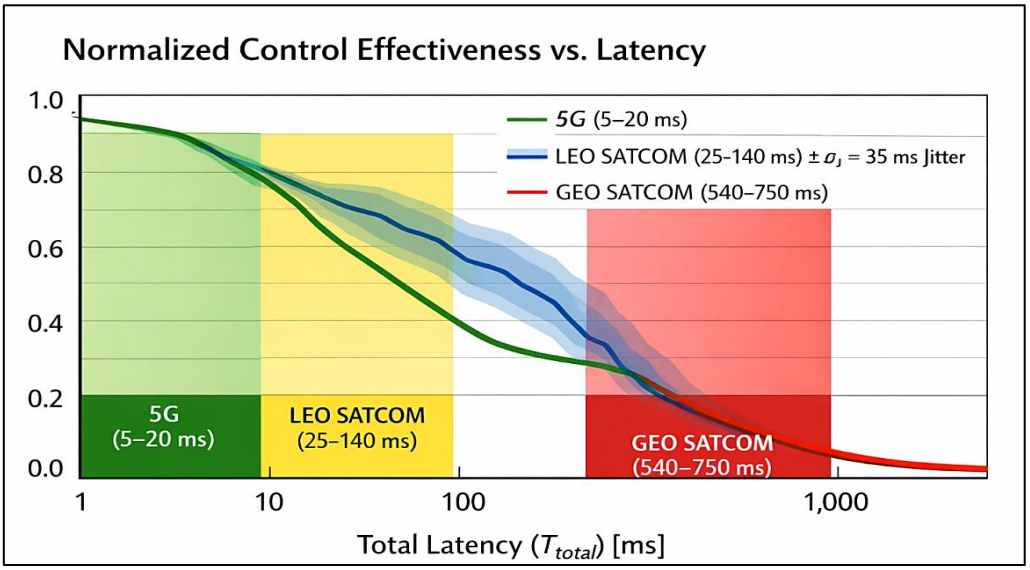

Figure 2. Normalised control effectiveness as a function of total communication latency for three operational scenarios. Shaded bands indicate characteristic latency ranges for 5G (5–20 ms), LEO SATCOM (25–140 ms), and GEO SATCOM (540–750 ms). Probabilistic confidence intervals derived from the stochastic jitter model (σ_J = 35 ms) are superimposed on the LEO band.

For the urban surveillance scenario at v = 15 m/s, the same LEO parameters yield $\Delta T_{a}^{max} \approx 620$ ms and Pbreach ≈ 7 × 10^{-9}, comfortably within the target. This confirms that LEO SATCOM is safe for low-speed urban teleoperation but requires autonomy-based mitigation at higher speeds. GEO SATCOM, operating with no effective margin in high-speed scenarios, has a Pbreach approaching 1.0 for disaster-response velocities, unequivocally requiring autonomous operation.

4.3. Mission Envelope Mapping

Figure 3 presents the mission envelope map, which maps the Zone A (Teleoperation Viable), Zone B (Supervised Autonomy Required), and Zone C (Full Autonomy Required) boundaries as a

© 2026 by the author(s). Distributed under a Creative Commons CC BY license.

Preprints.org (www.preprints.org) | NOT PEER-REVIEWED | Posted: 20 April 2026 doi:10.20944/preprints202604.1322.v1

function of communication latency and UAV velocity. The stochastic extension introduces probabilistic shading within Zone B, replacing the sharp boundary between supervised and full autonomy with a risk gradient characterised by Pbreach. As shown in Figure 3, GEO SATCOM confines teleoperable operations to below approximately 15 m/s, LEO SATCOM extends the operable envelope to approximately 40 m/s (with residual jitter risk above 25 m/s), and 5G links support teleoperation across the full UAV velocity range within coverage.

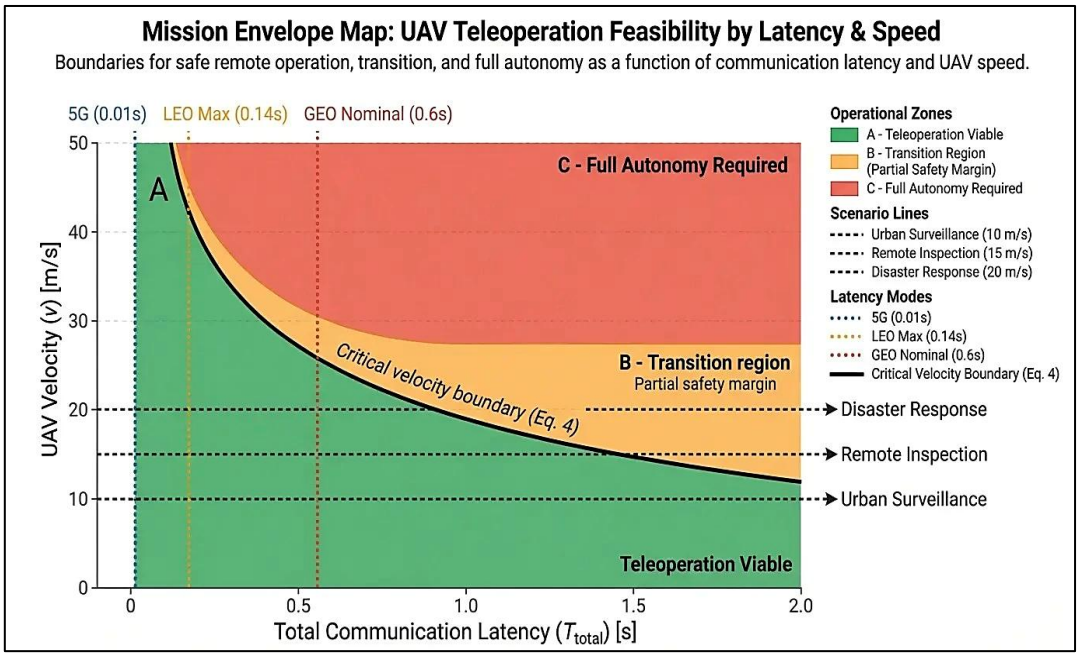

Figure 3. Mission envelope map showing Zone A (Teleoperation Viable), Zone B (Supervised Autonomy Required—with probabilistic shading indicating Pbreach gradient), and Zone C (Full Autonomy Required) as functions of total communication latency and UAV velocity. Boundaries are computed for d_{sao}^{e} = 30 m (urban baseline). Dashed lines indicate characteristic latency values for each communication mode.

5. Adaptive Autonomy Control Framework

5.1. Architectural Overview

The Zone A/B/C model of Section 4.3 provides a static operational map. In practice, communication quality varies continuously during flight as satellites rise and set, handovers occur, and atmospheric conditions change. The adaptive autonomy control framework (AACF) proposed herein transforms the static zone map into a dynamic control architecture in which the UAV monitors real-time link performance and adjusts its operational parameters accordingly. The architecture comprises three layers: a communication quality monitor, a zone classification engine, and an autonomy and velocity arbitrator.

The communication quality monitor measures T_{tota}^{L} and $\mathcal{J}$ in real time using round-trip probe packets transmitted at a rate sufficient to capture handover events without consuming significant link bandwidth. Measured values are passed to the zone classification engine, which computes the current Pbreach and assigns the UAV to Zone A, B, or C using the mission-specific thresholds derived in Section 3.4.

5.2. Dynamic Velocity Adjustment

When the measured Pbreach exceeds a configurable warning threshold $P^{W}{}_{a}{}^{rn}$, the autonomy and velocity arbitrator applies a dynamic velocity reduction to restore the latency safety margin. Velocity is adjusted according to:

© 2026 by the author(s). Distributed under a Creative Commons CC BY license.

Preprints.org (www.preprints.org) | NOT PEER-REVIEWED | Posted: 20 April 2026 doi:10.20944/preprints202604.1322.v1

$$v_{cmd} = \min(v_{desired}, d_{safe} / (T_{total,meas} + T_{human} + \Delta T_{safety})) \quad (9)$$

where $v_{desired}$ is the mission-desired velocity, $T_{total,meas}$ is the most recently measured round-trip latency, and ΔT_{safety} is a design safety buffer applied on top of the threshold. This equation ensures that the UAV never exceeds the critical velocity consistent with current link conditions, providing a continuous latency-aware speed limit rather than a discrete step-change.

5.3. Control Authority Transitions

When the zone classification engine transitions from Zone A to Zone B, the ground operator is notified through a graduated interface alert and control authority for local manoeuvres (obstacle avoidance, altitude hold, emergency stops) is progressively transferred to on-board autonomy. The operator retains authority for mission-level tasking—waypoints, payload activation, abort commands—but real-time flight control is delegated to the on-board system. This architecture is consistent with supervisory control principles established in the telerobotics literature [12].

Transition from Zone B to Zone C is triggered when Pbreach exceeds a critical threshold P^{crl}_{t} and the communication quality monitor indicates sustained link degradation rather than a transient handover event. In Zone C, the UAV executes a pre-planned contingency mission profile autonomously—which may include loitering at a safe altitude, proceeding to a recovery waypoint, or initiating a return-to-launch sequence—until link quality is restored. The transition logic is illustrated in Figure 4. All zone transitions are logged and available for post-flight analysis, supporting the empirical validation objectives described in Section 6.

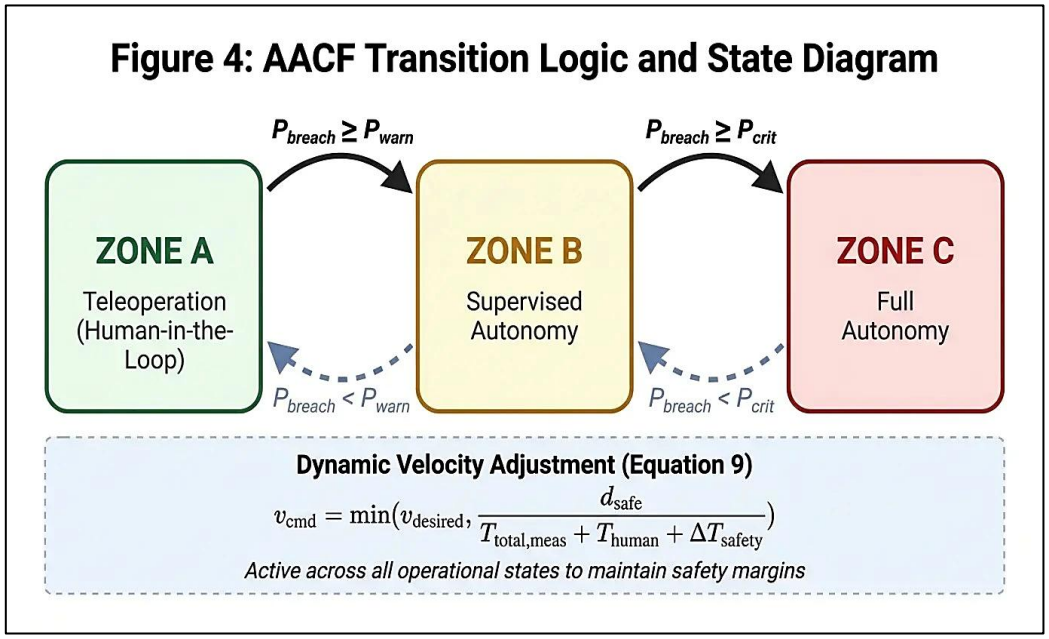

Figure 4. Adaptive autonomy control framework state diagram, illustrating the transitions between Zone A (Teleoperation), Zone B (Supervised Autonomy), and Zone C (Full Autonomy) as a function of measured Pbreach relative to warning ($P^{W}_{a}{}^{rn}$) and critical (P^{crl}_{t}) thresholds. Velocity adjustment (Equation (9)) operates continuously within all zones.

6. Empirical Validation Framework

6.1. Controlled Communication Emulation

While the analytical framework presented in Sections 3 and 5 is mathematically rigorous, practical adoption by system designers and certification authorities requires empirical evidence that the governing equations hold under realistic operating conditions. The proposed validation methodology employs a calibrated communication emulator—such as tc-netem under Linux or a

© 2026 by the author(s). Distributed under a Creative Commons CC BY license.

Preprints.org (www.preprints.org) | NOT PEER-REVIEWED | Posted: 20 April 2026 doi:10.20944/preprints202604.1322.v1

dedicated hardware emulator—inserted between the ground control station and a flight simulator. The emulator injects pre-defined latency profiles corresponding to GEO SATCOM (600 ms fixed), LEO SATCOM (80 ms mean with log-normal jitter, $\sigma\mathcal{J}$ = 35 ms), and 5G (10 ms fixed), enabling controlled experiments that vary communication conditions while holding all other experimental factors constant. In addition to nominal latency profiles, the emulator will be configured to inject worst-case sequence (WCS) handover events. These represent the 99th percentile (P_{99}) latency spikes were observed in LEO constellation data. This allows the framework to be tested against edge-case stochastic behaviour that standard log-normal distributions may under-represent.

6.2. Validation Goals

Three primary validation objectives are defined to bridge the gap between the analytical framework and operational reality.

- **Human Response Refinement**: The T_{human} constant, presently assumed at 250 ms, will be refined across pilot experience levels and stress conditions.
- **Cognitive Workload Mapping**: Participants drawn from trained UAV operators will provide a characterisation of perception-to-action delay under varying workloads. To support this, trials will incorporate the NASA Task Load Index (NASA-TLX) to provide a multidimensional rating of pilot cognitive workload, verifying if the transition to Zone B (Supervised Autonomy) successfully mitigates the mental demand associated with high-latency SATCOM links.
- **Control Effectiveness Verification**: The normalised control effectiveness curves of Figure 2 will be verified against actual pilot tracking error and obstacle avoidance performance data. This confirms whether the hyperbolic decay model accurately represents real operator behaviour across the latency range.
- **Stochastic Calibration**: The P_{breach} model will be calibrated against recorded handover events from LEO constellation data to refine the log-normal distribution parameters.
- **Operator State Sensitivity**: Following the trials, a sensitivity analysis will be performed on the T_{human} constant, varying it between 200 ms and 600 ms to demonstrate framework robustness to degraded operator states caused by fatigue or high-stress environments.

This validation programme is designed to generate a dataset that simultaneously confirms the theoretical framework and provides the empirical grounding required for regulatory engagement.

6.3. Flight Performance Indicators (FPIs)

To calibrate the control effectiveness curves and P_{breach} model, the following primary metrics will be recorded:

Table 3. Flight Performance Indicators (FPIs) for Empirical Validation.

Metric	Definition	Purpose
Tracking RMSE	Root Mean Square Error of 3D path deviation.	Quantifies precision loss as a function of T_{total}.
CASR (%)	Collision Avoidance Success Rate.	Validates safety boundaries in the Disaster Response scenario.
LRT (s)	Link Recovery Time.	Measures the latency in transitioning from Zone C back to Zone B.
Control Effort	Standard deviation of stick/control inputs.	Identifies pilot "over-control" or oscillation due to delay.

© 2026 by the author(s). Distributed under a Creative Commons CC BY license.

Preprints.org (www.preprints.org) | NOT PEER-REVIEWED | Posted: 20 April 2026 doi:10.20944/preprints202604.1322.v1

7. Regulatory Implications and Standards Consolidation

7.1. Current Regulatory Landscape

UAV regulation has advanced rapidly across major jurisdictions, with the European Union Aviation Safety Agency (EASA), the United States Federal Aviation Administration (FAA), and the International Civil Aviation Organization (ICAO) each publishing frameworks for UAS integration into non-segregated airspace [1]. However, current regulatory instruments focus primarily on airworthiness, operational approvals, and geofencing—they do not yet include quantitative communication performance requirements that link latency directly to allowable UAV speed, operational category, or required autonomy level. This gap is significant because, as BLOS operations expand, the absence of latency-aware standards creates ambiguity in safety cases and impedes the certification of SATCOM-dependent UAV systems.

7.2. Framework as Regulatory Input

The analytical framework presented in this paper is directly actionable as regulatory input. The autonomy transition threshold (Equation (5)) and the Pbreach metric (Equation (7)) together provide a quantitative basis for specifying minimum communication performance requirements as a function of UAV category, operational environment, and mission velocity. Table 4 maps the framework outputs to candidate regulatory requirements for three operational categories, providing a starting point for standards development. The comparative results across scenarios are shown in Table 4.

Table 4. Candidate Regulatory Requirements Derived from the Analytical Framework.

Operational Category	Max. Permissible $T_{tota}{}^{L}$ (ms)	Max. Pbreach Target	Required Autonomy Level	Applicable Comm. Mode
Low-speed urban (< 15 m/s)	750	$\leq 10^{-3}$	Zone A permissible	5G / LEO
Moderate-speed BLOS (15–40 m/s)	250	$\leq 10^{-5}$	Zone B minimum (supervised autonomy)	LEO / 5G
High-speed / safety-critical (> 40 m/s)	100	$\leq 10^{-6}$	Zone C (full autonomy)	LEO with jitter mitigation

Note: Values are derived from the framework of Sections 3–5 with $d_{sao}{}^{e}$ = 30 m and $T^{h}{}_{uva}{}^{n}$ = 250 ms. Regulatory adoption would require empirical validation as described in Section 6.

7.3. Pathway to Standards

Translating the framework into adopted standards requires engagement with ICAO Working Groups on UAS, EASA's U-Space regulatory track, and relevant standards bodies including EUROCAE WG-105 and the Radio Technical Commission for Aeronautics (RTCA) SC-228. The Pbreach metric is particularly well-suited to this process, as it maps directly onto the probabilistic safety objectives that underpin aviation certification under CS-UAS and EASA's Specific Assurance and Integrity Level (SAIL) framework [13]. Adoption would establish, for the first time, a quantitative linkage between satellite communication performance and UAV operational approval—a step that is both technically necessary and commercially significant as the BLOS UAV market matures.

8. Discussion

8.1. Communication Architecture Selection

The results of Section 4 confirm that GEO SATCOM, whilst indispensable for wide-area coverage, restricts human-in-the-loop teleoperation to low-speed regimes across all three operational scenarios. This finding reinforces the design principle that GEO-linked UAVs must be equipped with robust on-board autonomy as a primary—rather than fallback—capability [3,6]. LEO constellations

© 2026 by the author(s). Distributed under a Creative Commons CC BY license.

Preprints.org (www.preprints.org) | NOT PEER-REVIEWED | Posted: 20 April 2026 doi:10.20944/preprints202604.1322.v1

substantially expand the teleoperable envelope but require jitter mitigation strategies, including predictive handover scheduling and link quality monitoring, to reduce Pbreach to acceptable levels in high-speed scenarios. Hybrid architectures combining 5G and LEO SATCOM represent the most effective near-term solution, and the AACF of Section 5 provides a principled basis for managing the handover between these modes in flight.

8.2. System-Level Durability

It is important to emphasise that the framework operates at the system level and does not depend on the details of any particular communication technology. Advances in transponder efficiency, ground segment processing, or LEO constellation management will reduce individual latency components, but the fundamental relationship between propagation delay, jitter, and control effectiveness—governed by physics and human cognition—will persist [7,8]. The framework accommodates technological progress by parameterisation: updated latency values can be substituted into Equations (1)–(9) without altering the underlying structure. This durability is a critical property for a framework intended to inform long-lived regulatory standards.

8.3. Comparison with Existing Research

The deterministic thresholds derived herein are consistent with teleoperation research identifying round-trip delays of 300 to 500 milliseconds as the onset of significant performance degradation [12]. The introduction of Pbreach extends this finding by replacing the binary threshold with a risk metric directly usable in probabilistic safety assessment—an approach not previously applied to SATCOM-constrained UAV operations. The critical velocity metric (Equation (4)) similarly provides a concise operational parameter absent from existing UAV communication studies, enabling mission planners to translate latency specifications directly into permissible operational envelopes. Together, these contributions address analytical gaps identified across the UAV communication [2,3], networked control [12], and teleoperation [8] literatures.

9. Conclusions

This paper has presented a system-level analytical framework for latency-constrained UAV operations over SATCOM, comprising four integrated contributions: a deterministic latency decomposition model, a stochastic jitter extension yielding a probability of safety breach metric, an adaptive autonomy control architecture, and a regulatory implications analysis.

The principal findings are as follows. First, GEO SATCOM imposes round-trip delays that restrict safe teleoperation to below approximately 15 m/s in safety-critical scenarios. Second, LEO SATCOM substantially expands the operable envelope but introduces jitter-driven risk that, without mitigation, yields Pbreach values exceeding aviation safety targets at high speeds. Third, the adaptive autonomy control framework provides a practical, implementable architecture for managing these risks through real-time latency monitoring and dynamic velocity adjustment. Fourth, the framework maps directly onto candidate regulatory requirements for three operational UAV categories, providing actionable input for standards development.

The practical implications extend across UAV system design, communication architecture selection, and regulatory policy. For system designers, the critical velocity and Pbreach metrics provide quantitative specifications for on-board autonomy capability as a function of intended communication mode. For communication architects, the framework clarifies where GEO, LEO, and 5G links are appropriate and where hybrid architectures are required. For regulators, Table 3 offers a starting point for latency-aware operational approval criteria.

Future work should proceed in three directions. First, empirical validation through controlled flight trials with calibrated communication emulation, as outlined in Section 6, will refine the $T^{h}_{uva}{}^{n}$ constant and validate the Pbreach model against real pilot performance data. Second, the log-normal jitter model should be calibrated against measured LEO constellation performance data to reduce

© 2026 by the author(s). Distributed under a Creative Commons CC BY license.

Preprints.org (www.preprints.org) | NOT PEER-REVIEWED | Posted: 20 April 2026 doi:10.20944/preprints202604.1322.v1

distributional uncertainty. Third, formal engagement with ICAO, EASA, and RTCA working groups should translate the candidate requirements of Table 3 into adopted standards. This work constitutes a foundational step toward latency-aware UAV operation standards—a regulatory necessity that will grow only more pressing as unmanned systems are integrated into shared, complex airspace environments worldwide.

References

1. International Civil Aviation Organization (ICAO). *Unmanned Aircraft Systems (UAS)*; Circular 328-AN/190; ICAO: Montreal, Canada, 2011.
2. Gupta, L.; Jain, R.; Vaszkun, G. Survey of important issues in UAV communication networks. *IEEE Commun. Surv. Tutor.* **2016**, *18*, 1123–1152. https://doi.org/10.1109/COMST.2015.2495297
3. Zeng, Y.; Zhang, R.; Lim, T.J. Wireless communications with unmanned aerial vehicles: Opportunities and challenges. *IEEE Commun. Mag.* **2016**, *54*, 36–42. https://doi.org/10.1109/MCOM.2016.7470933
4. Barua, N. *SATCOM, the Future UAV Communication Link*. SSRN Electron. J. **2022**. https://doi.org/10.2139/ssrn.4059066
5. Barua, N. *Global Homeland Security Satellite Imagery Market: Strategic Outlook and Growth Trajectories*. SSRN Electron. J. **2025**. https://doi.org/10.2139/ssrn.5364419
6. Pratt, T.; Bostian, C.W.; Allnutt, J.E. *Satellite Communications*, 2nd ed.; Wiley: Chichester, UK, 2003.
7. Maral, G.; Bousquet, M.; Sun, Z. *Satellite Communications Systems*, 6th ed.; Wiley: Chichester, UK, 2020.
8. Hokayem, P.F.; Spong, M.W. Bilateral teleoperation: An historical survey. *Automatica* **2006**, *42*, 2035–2057. https://doi.org/10.1016/j.automatica.2006.06.027
9. del Portillo, I.; Cameron, B.G.; Crawley, E.F. A technical comparison of three low earth orbit satellite constellation systems. *Acta Astronaut.* **2019**, *159*, 123–135. https://doi.org/10.1016/j.actaastro.2019.03.040
10. Mozaffari, M.; Saad, W.; Bennis, M.; Nam, Y.-H.; Debbah, M. A tutorial on UAVs for wireless networks. *IEEE Commun. Surv. Tutor.* **2019**, *21*, 2334–2360. https://doi.org/10.1109/COMST.2019.2902862
11. Bhattacherjee, D.; Singla, A. Network topology design at 27,000 km/h. In *CoNEXT 2019*, Orlando, FL, USA, 2019; pp. 341–354. https://doi.org/10.1145/3359989.3365408
12. Sheridan, T.B. Telerobotics, Automation, and Human Supervisory Control; MIT Press: Cambridge, MA, USA, 1992.
13. Hespanha, J.P.; Naghshtabrizi, P.; Xu, Y. A survey of recent results in networked control systems. *Proc. IEEE* **2007**, *95*, 138–162. https://doi.org/10.1109/JPROC.2006.887288
14. National Academies of Sciences, Engineering, and Medicine. *Autonomy Research for Civil Aviation*; National Academies Press: Washington, DC, USA, 2014. https://doi.org/10.17226/18815
15. Khawaja, W.; Guvenc, I.; Matolak, D.W.; Fiebig, U.-C.; Schneckenburger, N. Air-to-ground channel modelling for UAVs. *IEEE Commun. Surv. Tutor.* **2019**, *21*, 2361–2391. https://doi.org/10.1109/COMST.2019.2917879

Disclaimer/Publisher's Note: The statements, opinions and data contained in all publications are solely those of the individual author(s) and contributor(s) and not of MDPI and/or the editor(s). MDPI and/or the editor(s) disclaim responsibility for any injury to people or property resulting from any ideas, methods, instructions or products referred to in the content.

© 2026 by the author(s). Distributed under a Creative Commons CC BY license.